Computational modeling of pore-scale fluid transport in realistic porous media

David J. Lopez Penha[*], Bernard J. Geurts[*],
Steffen Stolz[†,*] & Markus Nordlund[†]

[*]Dept. of Applied Mathematics
University of Twente, Enschede
The Netherlands

[†]Philip Morris International R&D
Philip Morris Products S.A., Neuchâtel
Switzerland

TransPore 2010, Villigen, Switzerland
August 19–20, 2010

Porous media: Filter application

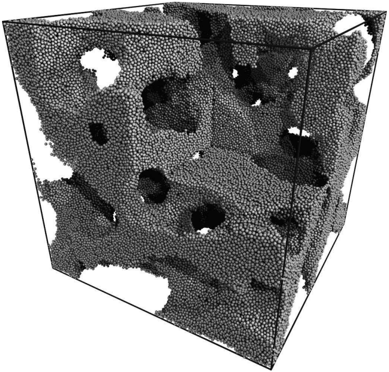

Source: `http://gubbins.ncsu.edu/research.html`

- Porous media may have complicated pore geometries
- Difficult to build practicable body-fitted grids

Porous media: Filter application

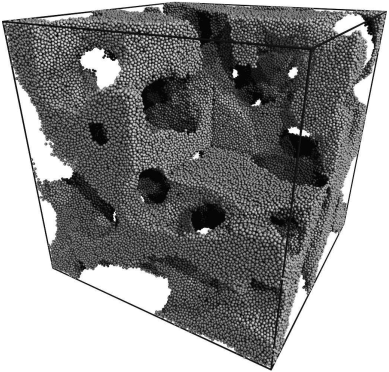

Source: `http://gubbins.ncsu.edu/research.html`

- Porous media may have complicated pore geometries
- Difficult to build practicable body-fitted grids

Goals

1. Develop "gridding-free" method for computing fluid transport in porous media
2. Method allows arbitrary pore geometries

Goals

1. Develop “gridding-free” method for computing fluid transport in porous media
2. Method allows arbitrary pore geometries

Outline

1. Modeling fluid transport in porous media
2. Validation
3. Application to realistic porous medium
4. Conclusions & outlook

Outline

Representing complex geometries

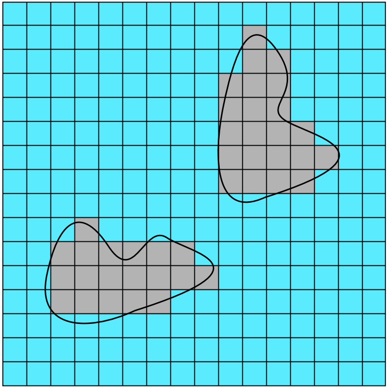

- Cartesian grid representation of fluid & solid domains
- Trade-off: High spatial resolutions — efficient numerical algorithms

Representing complex geometries

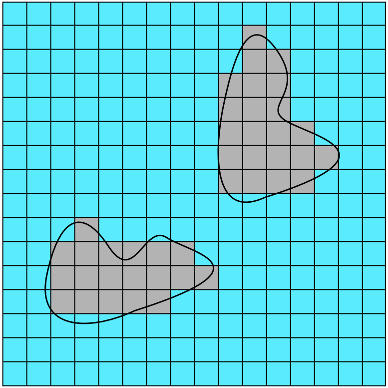

- Cartesian grid representation of fluid & solid domains
- Trade-off: High spatial resolutions — efficient numerical algorithms

Fluid dynamics

- Incompressible Navier-Stokes equations for fluid & solid domains:

$$\nabla \cdot \mathbf{u} = 0, \qquad \frac{\partial \mathbf{u}}{\partial t} + \mathbf{u} \cdot \nabla \mathbf{u} = -\nabla p + \frac{1}{\mathrm{Re}} \nabla^2 \mathbf{u} + \mathbf{f}$$

- Methodology: Immersed boundary method
- Force $\mathbf{f}$: Approximates no-slip condition (volume-penalization)

$$\mathbf{f} = -\frac{1}{\epsilon} \Gamma(\mathbf{x}) \cdot \mathbf{u}, \qquad \epsilon \ll 1$$

- $\Gamma(\mathbf{x})$: Phase-indicator function ($\Gamma = 1$ in solid; $\Gamma = 0$ in fluid)

Fluid dynamics

- Incompressible Navier-Stokes equations for fluid & solid domains:

$$\nabla \cdot \mathbf{u} = 0, \qquad \frac{\partial \mathbf{u}}{\partial t} + \mathbf{u} \cdot \nabla \mathbf{u} = -\nabla p + \frac{1}{\mathrm{Re}} \nabla^2 \mathbf{u} + \mathbf{f}$$

- Methodology: Immersed boundary method
- Force $\mathbf{f}$: Approximates no-slip condition (volume-penalization)

$$\mathbf{f} = -\frac{1}{\epsilon} \Gamma(\mathbf{x}) \cdot \mathbf{u}, \qquad \epsilon \ll 1$$

- $\Gamma(\mathbf{x})$: Phase-indicator function ($\Gamma = 1$ in solid; $\Gamma = 0$ in fluid)

Discretization

- Energy-preserving finite-volume method[1]
- Staggered grid (Cartesian & uniformly spaced)
- Implicit time-integration of force **f**

[1] R.W.C.P. Verstappen and A.E.P. Veldman, *J. Comput. Phys.*, **187** (2003)

Outline

Plane-Poiseuille flow

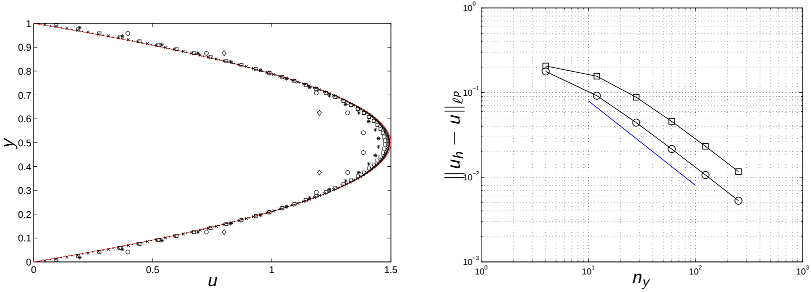

- $n_y = \{8, 16, \ldots, 256\}$, ℓ^p-norm of error ($p = \{2, \infty\}$)
- ($\bigcirc$)-marker $p = 2$; ($\square$)-marker $p = \infty$
- Velocity: Converges with order 1
- Similar behavior with Poiseuille flow in tube

UNIVERSITY OF TWENTE.

Plane-Poiseuille flow

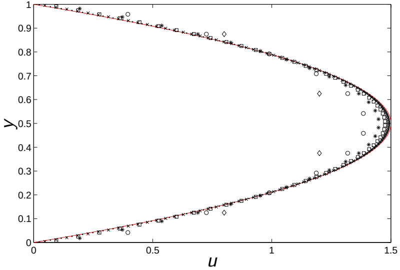

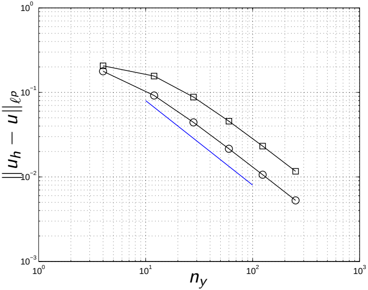

- $n_y = \{8, 16, \ldots, 256\}$, ℓ^p-norm of error ($p = \{2, \infty\}$)
- ($\bigcirc$)-marker $p = 2$; ($\square$)-marker $p = \infty$
- Velocity: Converges with order 1
- Similar behavior with Poiseuille flow in tube

Porous medium: Inline arrangement of squares

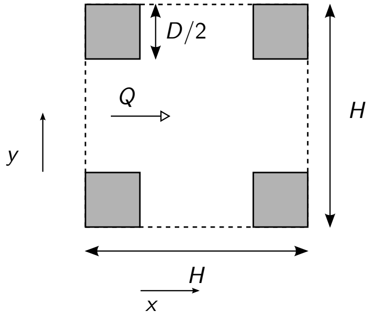

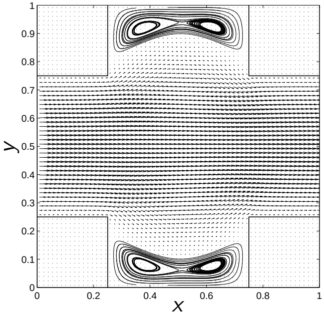

- Porosity: $\phi = 0.75 \Longrightarrow$ 25% solid grid cells
- Literature: A. Nakayama et al., *J. Heat Transfer*, **124** (2002)

Porous medium: Inline arrangement of squares

- Gradient average pressure $-\partial\langle p\rangle^f/\partial x$ vs. grid resolution:

$(n_x \times n_y)\backslash$Re	10	100	600
32×32	6.65	0.711	0.124
64×64	7.16	0.768	0.135
128×128	7.45	0.800	0.143
181 × 181 (Nakayama et al.)	**7.82**	**0.835**	**0.154**

Outline

1. Modeling fluid transport in porous media
2. Validation
3. **Application to realistic porous medium**
4. Conclusions & outlook

Realistic porous medium

- Porous medium: Primarily unidirectional fibrous material
- Geometric data: High-resolution 2D μCT-scans

Goal:

- Reconstruct from 2D-scans a 3D digitized porous block
- Simulate velocity & pressure fields, extract quantities of interest: $\mathbf{u}_{\text{max}}$, macroscopic pressure gradient, permeability

Realistic porous medium

- Porous medium: Primarily unidirectional fibrous material
- Geometric data: High-resolution 2D μCT-scans

Goal:

- Reconstruct from 2D-scans a 3D digitized porous block
- Simulate velocity & pressure fields, extract quantities of interest: $\mathbf{u}_{\text{max}}$, macroscopic pressure gradient, permeability

Source data: 2D μCT-scans

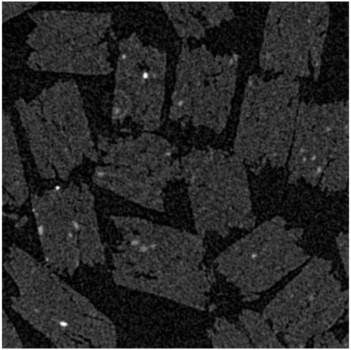

- Data: 8-bit, gray-scale images [resolution $= (512)^2$ pixels]

Map to black & white

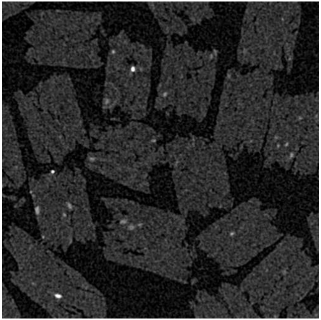

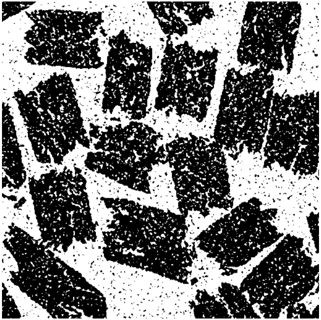

- Black = Solid domain, $\Gamma(\mathbf{x}) = 1$
- White = Fluid domain, $\Gamma(\mathbf{x}) = 0$

Noise reduction

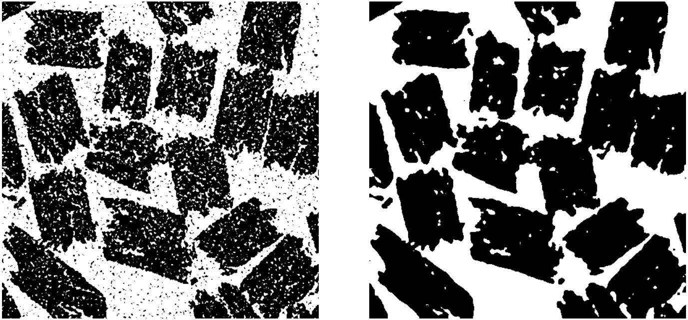

- Spatial filter: Uniform weights, filter width = 7 pixels
- Unavoidable smoothing of solid edges

Cartesian grid representation

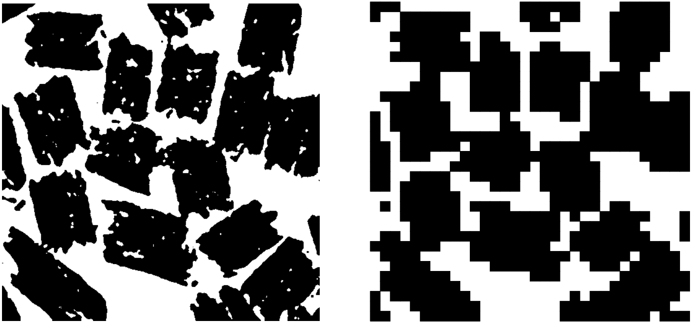

- Left: Processed (high-resolution) μCT-image
- Right: Cartesian grid representation using $\Gamma(\mathbf{x})$ [grid $= (32)^2$]

Cartesian grid representation

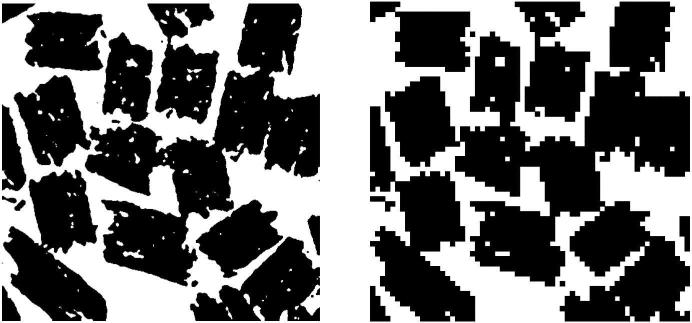

- Left: Processed (high-resolution) μCT-image
- Right: Cartesian grid representation using $\Gamma(\mathbf{x})$ [grid $= (64)^2$]

Cartesian grid representation

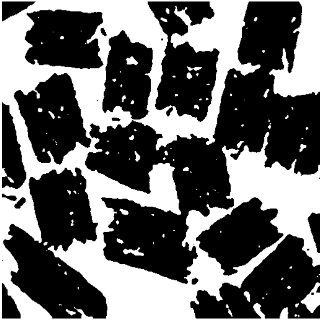

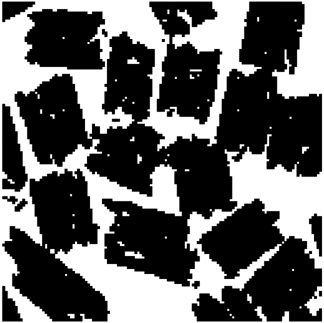

- Left: Processed (high-resolution) μCT-image
- Right: Cartesian grid representation using $\Gamma(\mathbf{x})$ [grid $= (128)^2$]

3D representation & velocity field

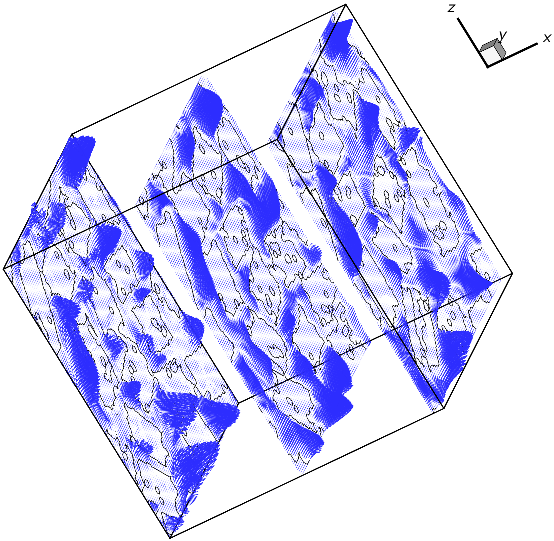

Numerical results: Scalar convergence

- Scalar system properties vs. grid resolution (at $\mathrm{Re} = 1$):

	ϕ	$u_{\mathrm{max}}/\lvert\langle\mathbf{u}\rangle\rvert$	$-\partial\langle p\rangle^f/\partial x = 1/k_x$
$(32)^3$	0.4077	14.2290	5.326E+03
$(64)^3$	0.4131	20.1634	7.961E+03
$(128)^3$	0.4131	23.1023	9.862E+03

Numerical results: Planar velocity convergence

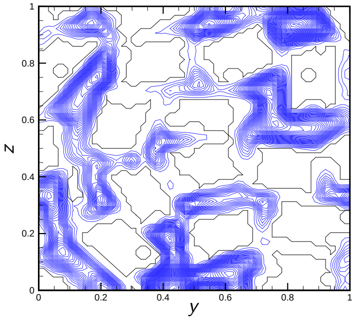

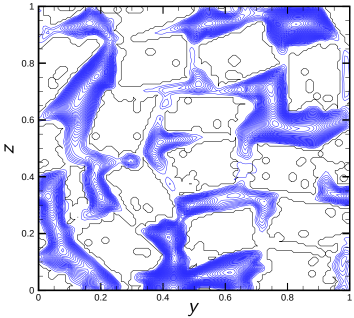

- Out-of-plane velocity component
- Left: Grid resolution $= (64)^2$, Right: Grid resolution $= (128)^2$

Numerical results: Pointwise velocity convergence

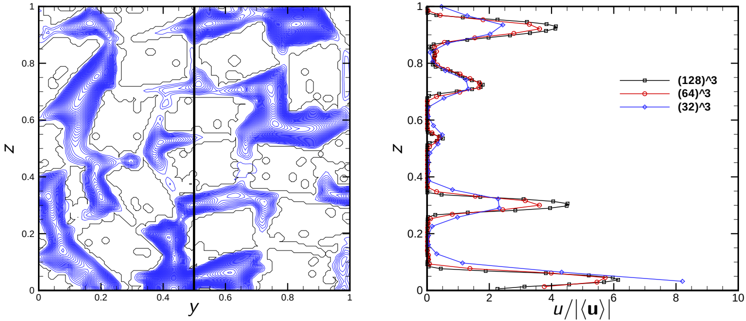

- Streamwise velocity vs. grid resolution ($x = y = 0.5$, $\mathrm{Re} = 1$)

Outline

Conclusions & outlook

Conclusions:

- Immersed boundary method can include arbitrarily shaped solid objects
- Immersed boundary method can readily describe qualitatively laminar fluid dynamics
- Quantitatively accurate results require high spatial resolutions

Outlook:

- Improve order of convergence of immersed boundary method
- Extend method to incorporate heat & mass transfer

Conclusions & outlook

Conclusions:

- Immersed boundary method can include arbitrarily shaped solid objects
- Immersed boundary method can readily describe qualitatively laminar fluid dynamics
- Quantitatively accurate results require high spatial resolutions

Outlook:

- Improve order of convergence of immersed boundary method
- Extend method to incorporate heat & mass transfer